XANES spectroscopy on iron(II) complexes

Raffaele Salvia[1]

[1]Scuola Normale Superiore, Pisa(PI), Italy
[1]University of Pisa, Pisa(PI), Italy

September 5, 2018

Contents

1 Introduction

In this project, I tried to calculate the X-ray absorption spectra of two classes of molecules: iron bipyridines and iron carbenes.

These molecule are studied because of their potential utility for a photovoltaic technology called *dye-sensitized solar cells* (DSCs). In dye-sensitized solar cells, a *photosynthesizer* material can convert sunlight into energy ceding electrons to a semiconductor (usually TiO_2).

1. The photosynthesizer material must be able to eject an electron when hit by photons, giving it to the semiconductor (*electron injection*);
2. *Charge recombination* has to be avoided, that is, the injected electron must not return at its original place;
3. The photosynthesizer molecule has to be able to fire again in a short time (*regeneration*);

All the existing models of DSCs employ rare and expensive elements, mainly ruthenium. Iron is in the same group of ruthenium, and it is much cheaper, but so far no efficient iron photosynthesizer complexes has been realized. The most efficient photosynthesizer molecules currently on the market are ruthenium(II) polypyridines. The most natural choice for trying to build an iron-based photosynthesizer complex are thus the iron(II) polypiridines. Research in this area started in the late 1990s[1], and some progresses have been made, but Fe(II) polypyridines remain with a low injection power. Carbenes are a promising and recently appeared class of molecules, which can efficiently inject electrons into a TiO_2 layer. Unfortunately, carbenes exhibit also a fast charge recombination[2] .

XANES is the acronym for "X-ray Absorption Near Edge Spectroscopy".
The quantity we want to predict is the absorption coefficient $\mu(E)$ of X-rays on materials; it is defined with the relation

$$I = I_0 e^{-\mu x} \ , \tag{1}$$

where I is the intensity of the X-ray after it has traveled a distance x inside the material. As the energy of the incoming photon reaches the value required to excite an electron, the absorption coefficient has a sharp increase. We call it an *absorption edge*. We call K, L, M, ... the edges relatives to transitions which displace an electron from the $n = 1$, $n = 2$, $n = 3$ ... energy levels. Before and after the edge, the spectrum has some irregular features, the *near-edge structure*. These are determined by the environment in which the atom is posed (that is, the surrounding atoms). Therefore, studying the XANES spectra can reveal useful information about the molecule.
I worked with the K edge, that is, the transitions which involve an $1s$ electron. The first empty level in the iron atom which the $1s$ electron can reach with a dipole transition is the $4p$ orbital. The transition $1s \to 4p$ occurs at about 7112 eV in unperturbed Fe atoms; so the K edge of iron complexes will be at about this energy. There are $3d$ empty

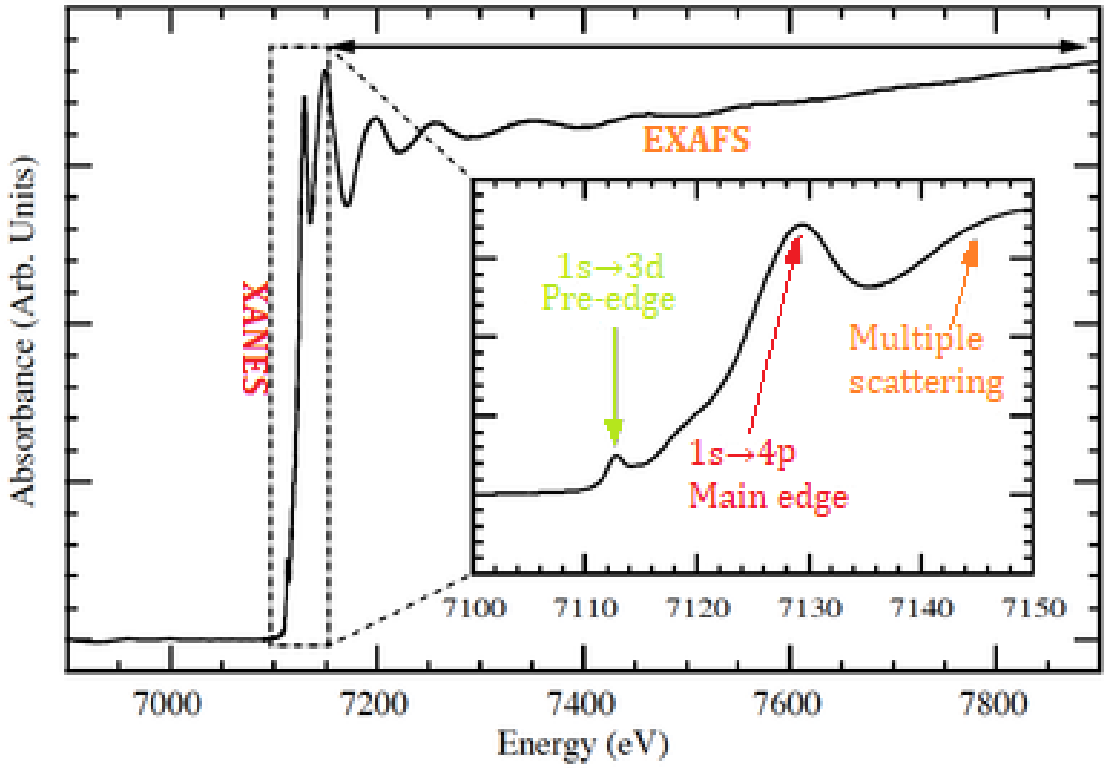

Figure 1: Subdivision of an X-ray absorption spectrum

orbital before, which can be reached with a quadrupole transitions; this gives origin to the *pre-edge* features.
If the energy of the photon is bigger than the binding energy of the $1s$ electron, this electron will escape the iron atom. If there were no surrounding atoms, the electron would escape away; but in a molecule this electron will be scattered by the other atoms, and it can return back to the iron $4p$ orbital. This is the reason for which the XANES spectra have more maximums after the main edge.

2 Theory

The oscillations after the absorption edge would not be present if the atom were isolated. They arise from the interaction of the emitted electron with the surrounding atoms, which can scatter the electron back to its atom. We can express absorption coefficient $\mu(E)$ as

$$\mu(E) = \mu_0(E)[1 + \chi(E)] \tag{2}$$

where $\chi(E)$ is the absorption amplitude from this back-scattering process. The Fermi Golden Rule for periodic perturbations tells us that the probability of an electron to pass from a bound state $|i\rangle$ to a continuum state $\langle k|$ is proportional to the matrix element of

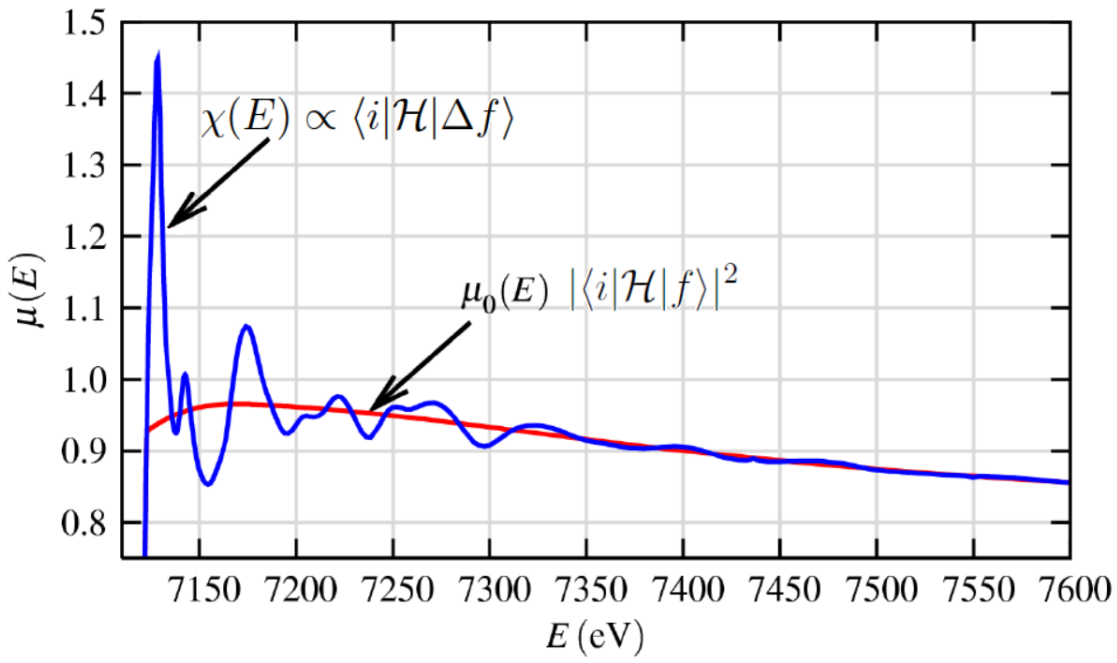

Figure 2: Definition of the $\chi(E)$ function (from [3])

the perturbation between the two states:

$$\mu(E) \propto \langle f|\mathcal{H}|i\rangle \tag{3}$$

The final state of the photoelectron will be perturbed by the presence of the surrounding atoms. Let $\langle f| = \langle f_0| + \langle \Delta f|$, where $\langle f_0|$ is the unperturbed final state. Replacing in equation 3 and keeping the first order, we have

$$\mu(E) \propto |\langle f_0|\mathcal{H}|i\rangle|^2 \left[1 + \frac{\langle \Delta f|\mathcal{H}|i\rangle \langle f_0|\mathcal{H}|i\rangle^*}{|\langle f_0|\mathcal{H}|i\rangle|^2} + h.c.\right] \tag{4}$$

We can identify equation 4 with the equation 2, with

$$\chi(E) \propto \langle \Delta f|\mathcal{H}|i\rangle \tag{5}$$

We can derive an analitical expression for the function χ by means of some rough approximations. The initial state $|i\rangle$ can be treated as a Dirac delta. In the minimal couping, the interaction term is $\mathcal{H} \sim \vec{p} \cdot \vec{A}$, which for a plane wave is proportional to $e^{i\vec{k}\cdot\vec{r}}$. If we call ψ_f the wavefunction of the scattered electron, we can write the matrix element as

$$\chi(E) \propto \int \mathrm{d}r \delta(r) e^{ikr} \psi_f(r) = \psi_f(0) \tag{6}$$

Thus, χ is proportional to the amplitude of the wave function of the scattered electron at the original atom. We can approximate the propagator of the electron with a outward

spherical wave ($\psi(k,r) = \frac{e^{ikr}}{kr}$). The electron has to travel until the second atom, get scattered (getting some unknown factor $f(k)$ and some phase change $\theta(k)$), and to return back to the original atom. That is, absorbing the factors in the $f(k)$,

$$\chi(k) = \frac{e^{ikR}}{kR}[kf(k)e^{i\theta(k)}]\frac{e^{ikR}}{kR} + h.c. = \frac{f(k)}{kR^2}\sin(2kR + \theta(k)) \tag{7}$$

Summing over the neighboring atoms, and adding a term to account for the thermal agitation, we finally obtain

$$\chi(E) = \sum_{atoms} \frac{f_j(k)}{kR_j^2}\sin(2kR_j + \theta_j(k))\, e^{-2k^2\sigma_j^2} \tag{8}$$

The approximations made to derive equation 8 are no more valid in the region immediately after the edge. For this reason, 8 applies only to the EXAFS region. While the oscillating behavior is still qualitatively correct, there is not a such simple formula for predicting the spectrum in the XANES region, where the absorption is influenced by a wide variety of different effects. For this reason, analyzing the XANES region could reveal a lot of information, if we found ways to relate some features of the XANES spectrum to some properties of the molecule under investigation.

3 Methods

Throughout all the project, I employed the *FDMNES* program by Y. Joly[**?**][4]. This program accepts as an input a file containing the coordinates of the atoms, and returns as output several files (depending on the input options).

3.1 General options

The program allows to use two methods to calculate the XANES spectrum: the *Muffin Tin* method and the Finite Difference Method.
In the Muffin Tin approximation, the potential is replaced by a constant outside a certain distance from the atoms. Inside the atoms, then, the potential is made spherically symmetric. These simplification allow the problem to be solved by means of Green Functional. The Finite Difference Method, whence *FDMNES* takes its name, allows instead an arbitrary potential. In this method, the Schrödinger equation is reduced to a linear system, taking a discrete second derivative. Another option of the program is to use Time Dependent Density Functional Theory (TDDFT) to calculate the potential. The Finite Difference Method takes considerably more time than the Muffin Tin Method, but it yielded better results in all the calculations I have done. In the remaining part of this report I shall talk only of the results of the FD method.

3.2 Input structures

The program is very sensitive to the structure of the molecule in input, like the real XANES spectra it seeks to model.
I used some crystallographic structures (*.cif* files), and some structures calculated using Density Functional Theory. *FDMNES* can handle the list of atomic coordinates in two ways:

- with the *Molecule* options, the software assumes that the specified atoms are the only ones present;
- with the *Crystal* options, the software interprets the input as a cell in a lattice, and replicates it.

After some tries, I stuck with the *Molecule* option; however, better results are obtained including in the input the surrounding molecules in the actual crystallographic structure. In the rest of the report, I shall refer to this option as *shell molecule*. The program simulates a sphere centered in the absorbing atom. The output usually converges with radiuses bigger than 6 Å. Enlarging further the size of the cluster increases dramatically the time required by the calculation.

3.3 Convolution

Once we have computed the transition probability for every energy, there remains one final step for us to be able to confront with the experimental spectrum: the convolution. The program *FDMNES* does it automatically, but I tried to perform the broadening on my own. There are two decisions that are to be made:

- Where is the Fermi energy, below which the transition probability has to be 0, because final states are already occupied;
- Selecting the width $\Gamma(E)$ of the convolving Lorentzian (we do not convolve with Gaussians, assuming the thermal effects to be negligible)

The program estimates the Fermi Energy case by case, with a non self-consistent procedure.
The broadening $\Gamma(E)$ can not be smaller than the width of the core-hole state of the iron atom without an 1s electron, which is $\Gamma_{CH} = 1.33$ eV [4]. In addition to this, there is additional broadening due to the inelastic scattering of the ejected electron. The program model this with the following formula:

$$\Gamma(E) = \Gamma_{CH} + \Gamma_m \left(\frac{1}{2} + \frac{1}{\pi} \arctan \left(\frac{\pi}{3} \frac{\Gamma_m}{E_{larg}} \left(\epsilon - \frac{1}{\epsilon^2} \right) \right) \right) \ , \ \epsilon = \frac{E - E_F}{E_{cent}} \tag{9}$$

The program uses the constants $\Gamma_m = 15$ eV, $E_{cent} = 30$ eV, $E_{larg} = 30$ eV and $\Gamma_{CH} = 1.25$ eV for the K. edge of iron. I will call this one the *default convolution*.
In the experimental data, there are never sharps features in the EXAFS region (from

~40 eV after the main edge): it is necessary to have a broadening of at least ~10 eV to remove them from the raw absorption spectrum. On the other hand, in the near-edge region the additional broadening does not always improve the agreement with the experimental data. Therefore, sometimes I convolved with constant Γ_{CH} in the near edge region: I will refer to this as the *core-hole convolution*.

4 Bipyridine series

4.1 $[Fe(bpy)_3]^{2+}$

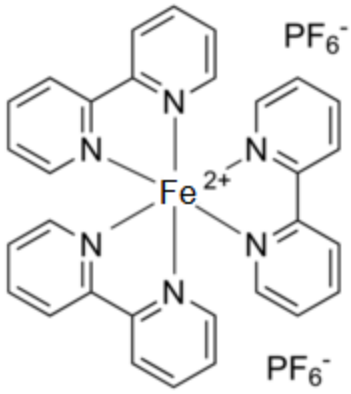

Figure 3: Structural formula of iron(II) tris-(2,2')bipyridine hexafluorophosphate

I made the greatest part of my test calculation on a crystallographic structure of the molecule $[Fe(bpy)_3](PF_6)_2$. As seen in figures 4 and 5, using the core-hole convolution I obtained a spectrum with the correct features; but the ratio between the first and the second peak of the spectrum is bigger than the experimental one. I investigated the effect of moving electrons from the N atoms of the ligands to the Fe atom (figure 7). The main effect is that the height of the first peak changes. The ratio between the heights of the two peaks is somewhat linear as a function of the net charge on the Fe atom, with some outliers. The slope depends on the internal configuration. The internal configuration of the other atoms, on the other hand, does not seem to affect the predicted spectrum.

Changing the configuration, sometimes the pre-edge becomes unnaturally big. In these cases, moving up the Fermi Energy can be used to nullify the transition.

Unique among the molecules of this series, the spectrum of iron tris-bipyridine owns a shoulder in its main edge. This feature is predicted by the program only if we include the $[PF_6]^-$ anions in the input structure: including only the $[Fe(bpy)_3]^{2+}$ molecule in the cluster, it results in an unbroken edge. However, if we replace the $[PF_6]^-$ anions with $[SO_4]^{2-}$, the shoulder does not change.

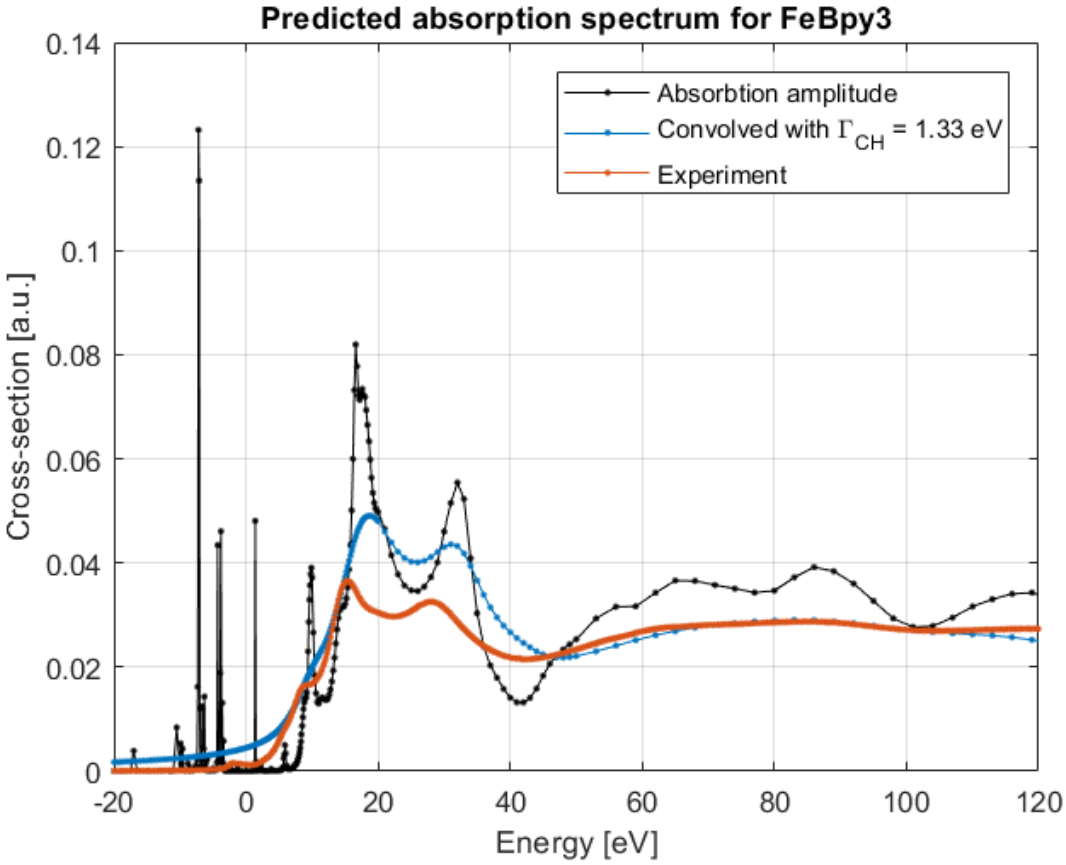

Figure 4: Default convolution of the spectrum of $[Fe(bpy)_3]^{2+}$

4.2 $Fe(bpy)_2(CN)_2$

I employed a crystal structure of $Fe(bpy)_2(CN)_2$ hydrate. The muffin tin method fails to predict the separation between the two peaks. Using the finite difference method and the default convolution, the calculated spectrum is instead fairly close to the measured spectrum. Moving electrons from the $4s$ to the $3d$ orbital, the first peak can be adjusted to match better the experimental data. The pre-edge inflates only occasionally.

4.3 $[Fe(bpy)(CN)_4]^{2-}$

For this molecule I had a crystallographic structure of $K_2[Fe(bpy)(CN)_4]$. The calculations based only on $[Fe(bpy)(CN)_4]^{2-}$ completely fail to predict the actual spectrum. Even including the K^+ anions, the amplitudes of the peaks are much smaller than in the experiment. Only if we include the molecular shell, we get a prediction qualitatively right.

Changing the internal configuration of the Fe atom would not alter a lot the peaks, but it would destroy the double feature in the pre-edge.

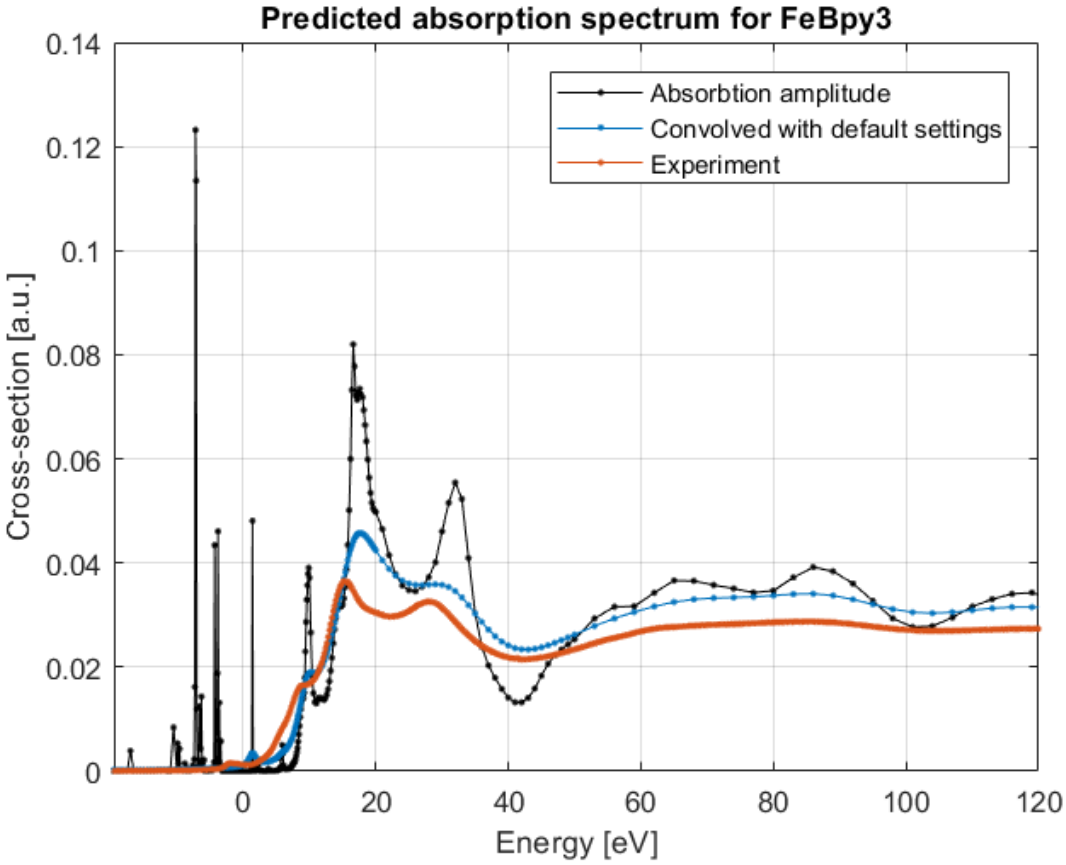

Figure 5: Core-hole convolution of the spectrum of $[Fe(bpy)_3]^{2+}$

4.4 $[Fe(CN)_6]^{4-}$

The two-peaks shape of the absorption spectrum of $[Fe(CN)_6]^{2+}$ depends on the presence of two shells of atoms around the central Fe atom. The predicted spectra of a "toy octahedron" FeC_6 possesses indeed only one peak.

The real structure I used was a crystallographic structure of $K_4[Fe(CN)_6]$, the same substance analyzed in the experimental data.

Using the core-hole convolution (see section 3.3), the predicted spectrum has the right features at the right places, but the heights of both peaks are too big. Figures 13, 14, 15 and 16 show the results of charge transfers between the central atom, the C shell and the N shell. As electrons move to the center, the first peak becomes lower, while the second peak is substantially unchanged (some tries with fictional molecules make me think that the second peak does depend on the distance between the iron atom and the ligands). This dependence of the first peak by the electronic configuration suggests that the corresponding transition amplitude depends on the value of the potential in the central atom, coherently with equation 6.

The only way to change the altitude of the second peak is to change the convolution.

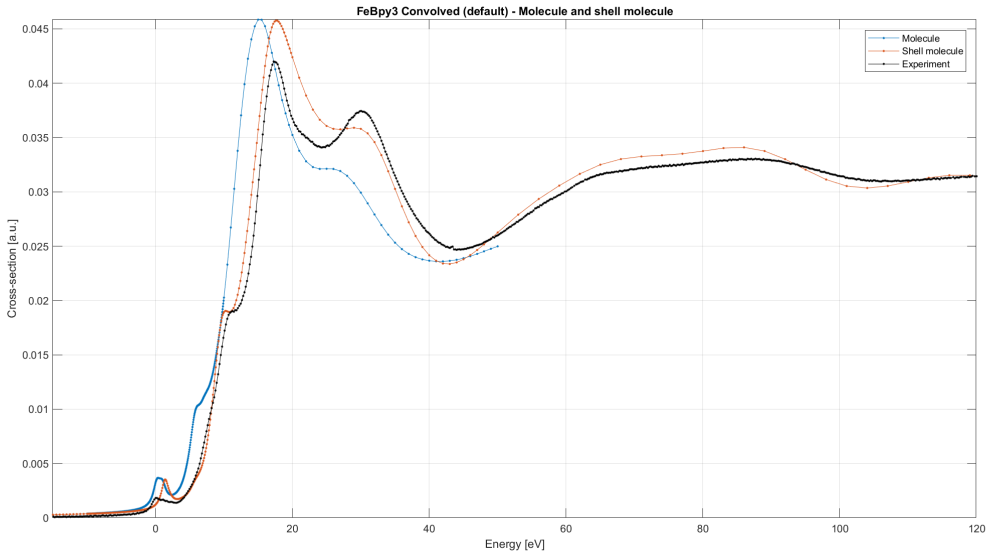

Figure 6: Predicted and experimental spectra for $[Fe(bpy)_3]^{2+}$

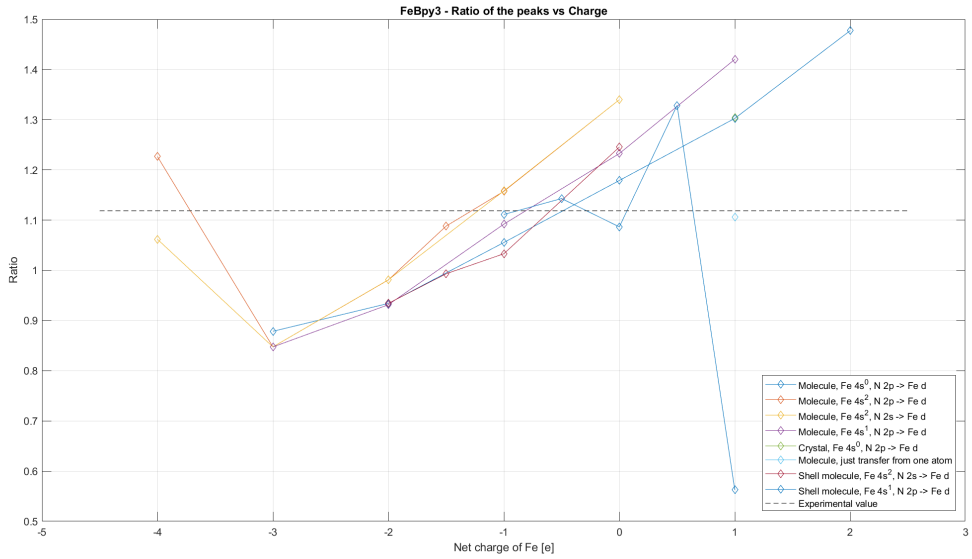

Figure 7: Ratio between the first and the second peak of the $[Fe(bpy)_3]^{2+}$, for various electronic configurations

The default convolution of the FDMNES program (figure 17), which takes account of the inelastic processes, produces indeed a much better agreement with the experimental spectrum.

Using this convolution, the predicted amplitude of the first transition is a bit lower than real; this could be adjusted by some minor displacement of electrons from the Fe

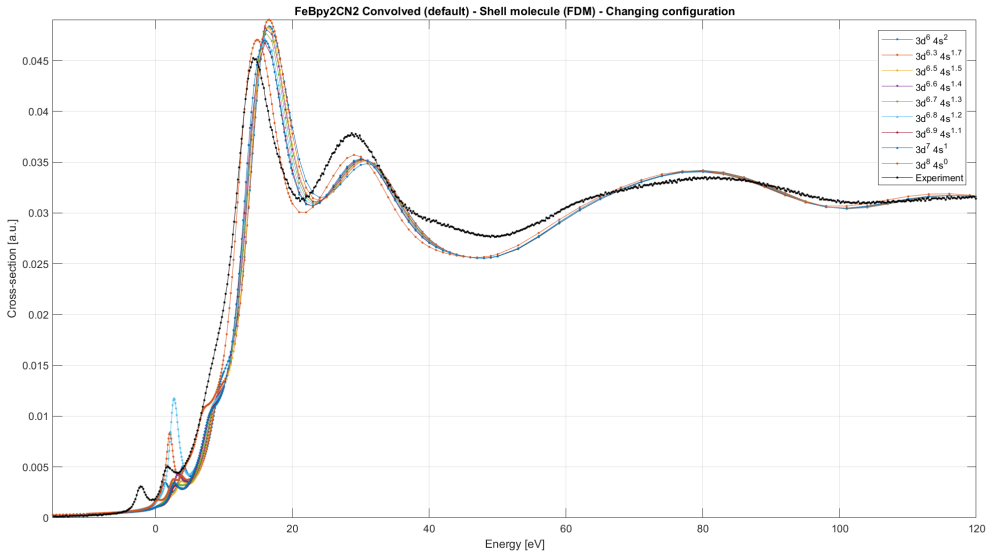

Figure 8: Predicted and experimental spectra for $Fe(bpy)_2(CN)_2$

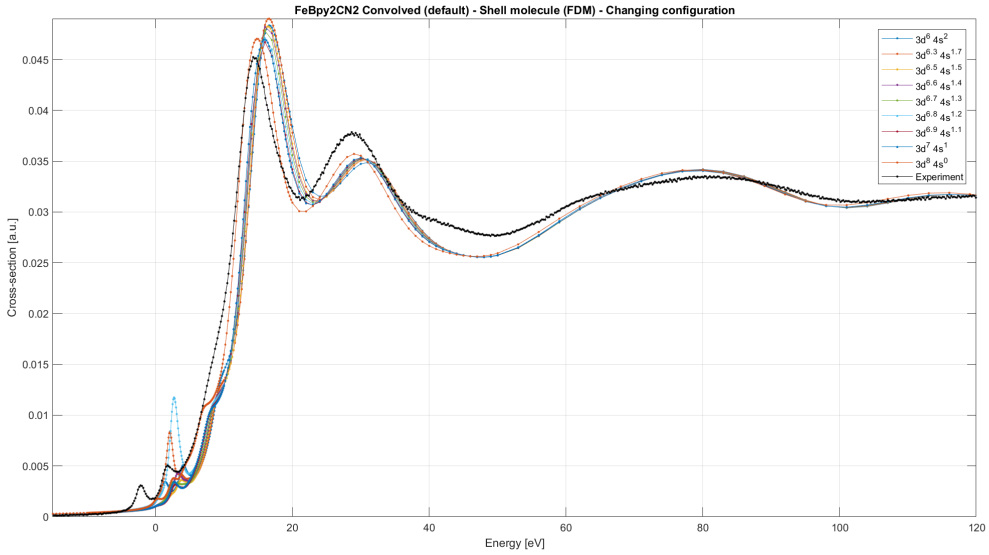

Figure 9: Predicted and experimental spectra for $Fe(Bpy)_2(CN)_2$

atom to the CN groups.

4.5 Whole series

The experimental spectra of all the molecules in this family, shown in figure 18, cross in several nodal points. The spectra of the intermediate compounds can be viewed as a sort

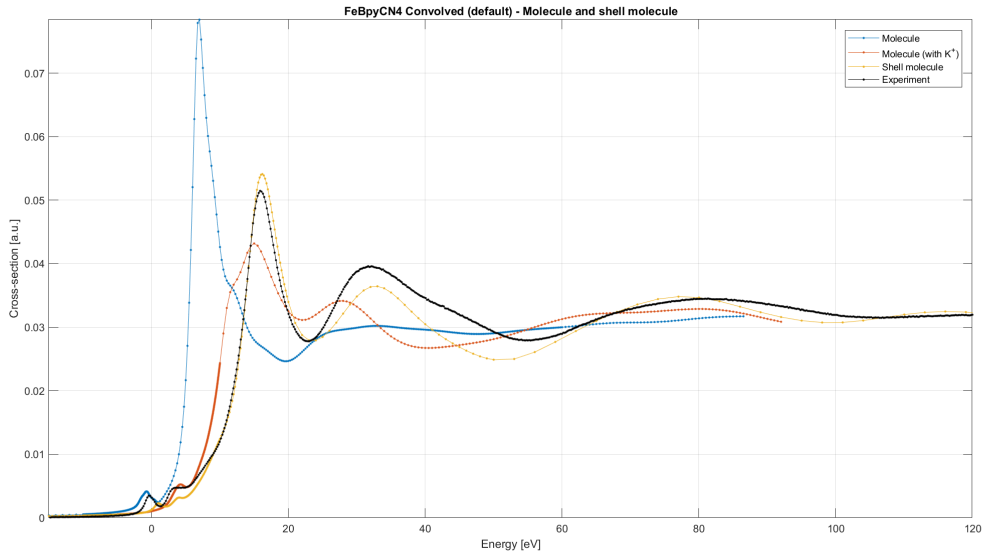

Figure 10: Predicted and experimental spectra for $[Fe(bpy)(CN)_4]^{2-}$

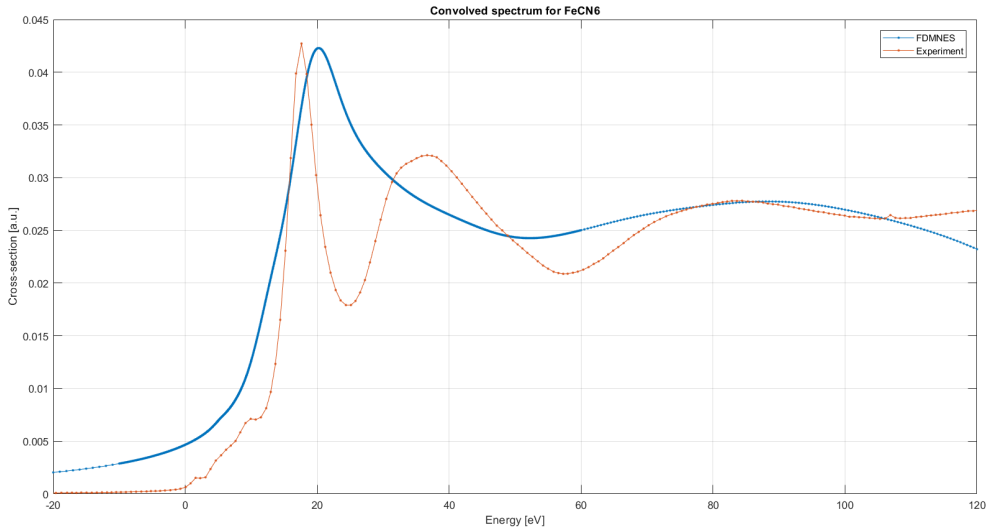

Figure 11: Predicted spectrum of the software for an hypothetical FeC_6

of linear combination of the spectra of the iron bipyridine cation and of the ferrocyanide anion, even if this is not a perfect description.

With the single molecules as input, the computed spectra fail to cross at nodal point, because their edges are at different energies. With an artificial alignment, three of them can be made to cross, but not $[Fe(bpy)(CN)_4]^{2-}$. Adding the K^+ cations to the latter (figure 19), the spectrum does cross with the other three, but at the wrong point: in

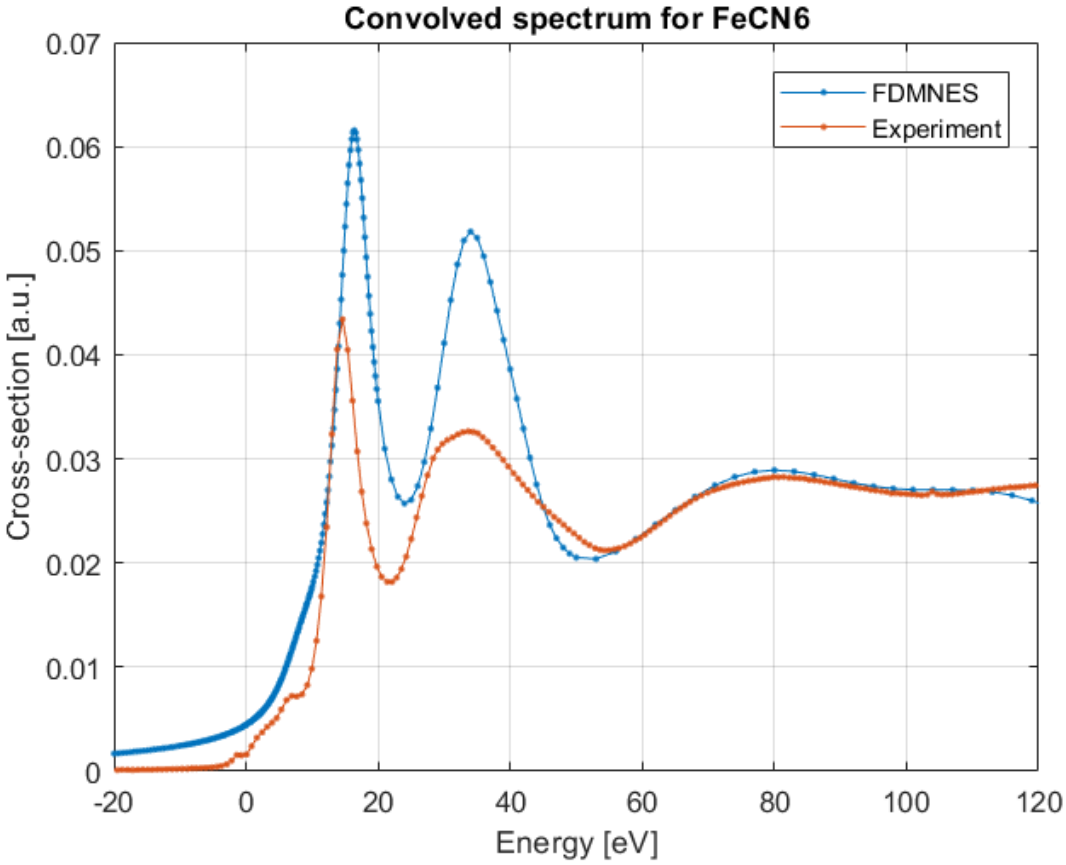

Figure 12: Predicted spectrum for $[Fe(CN)_6]^{4-}$

particular, the second nodal point should occur after the first peak and not before. Moreover, the relative intensities of the peak do not correspond to the experimental data.

Including the shell of surrounding molecules (figure 20), the predicted spectra look very similar to the experiment. With the core-hole convolution (figure 21), we have a better shape for $[Fe(bpy)_3]^{2+}$, but the amplitude of the XANES region is overestimated. In figure 22, I modified the configuration of $[Fe(bpy)_3]^{2+}$ and $Fe(bpy)_2(CN)_2$, in order to get closer to the experimental data.

5 Carbene series

5.1 $[Fe(terpy)_2]^{2+}$

For, iron terpyridine -the compound drawn in figure 23- I tested the structures produced by two DFT functionals (PBE and BLYP), as well as a crystallographic structure of $Fe(Terpy)_2(ClO_4)_2$, and plotted the results in figure 24. The BLYP structure does not resemble much the experiment. The PBE structure and the shell molecule produce

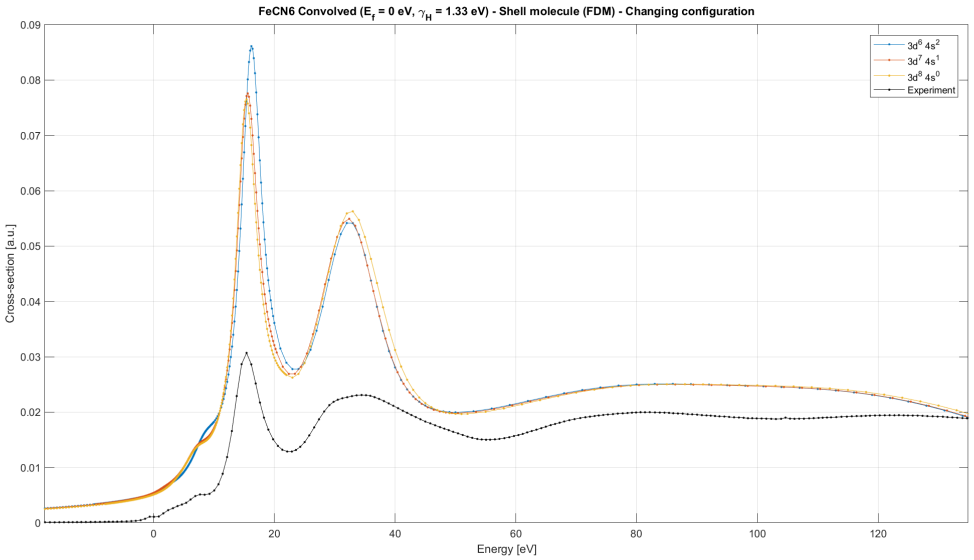

Figure 13: Effects of changes of the internal configuration of the absorbing atom on the predicted $[Fe(CN)_6]^{4-}$ spectrum

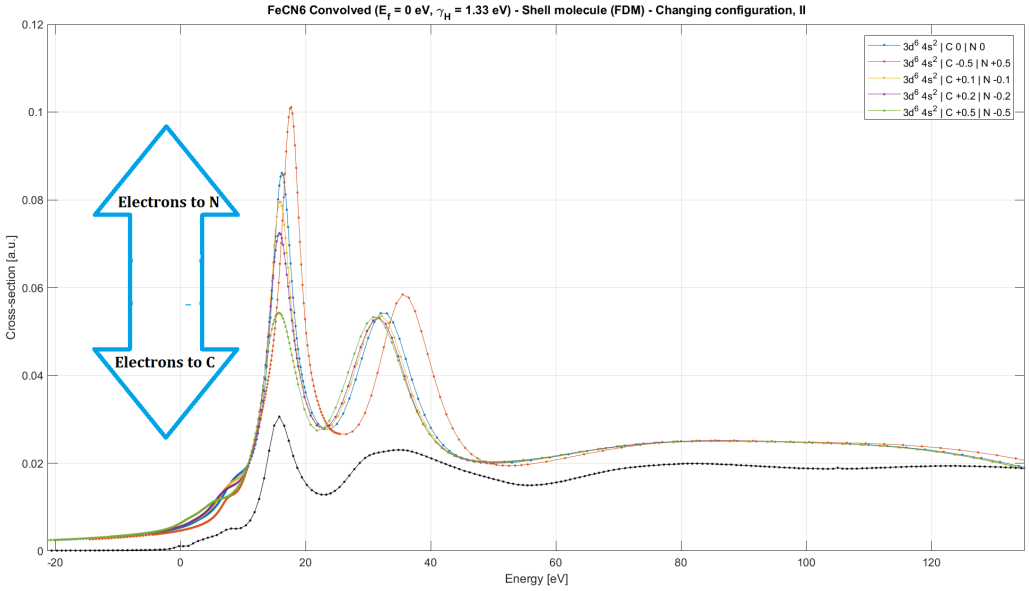

Figure 14: Effects of charge transfer between N and C on the predicted $[Fe(CN)_6]^{4-}$ spectrum

similar results, provided that we include the anions. Like for iron bipyridine, the ratio between the peaks varies linearly with the charge on the Fe atom, as shown in figure 25.

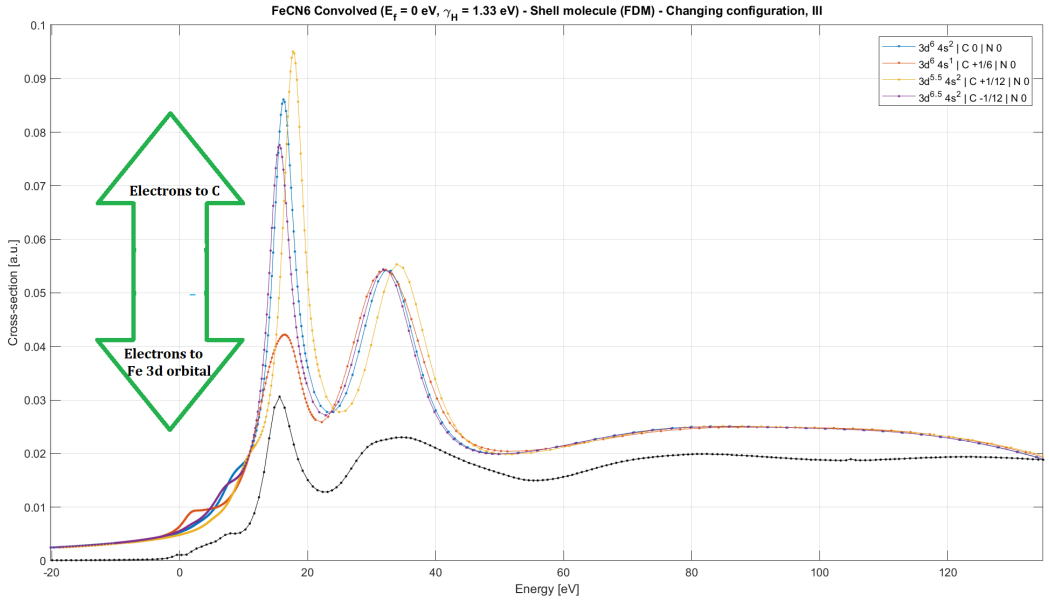

Figure 15: Effects of charge transfer between C and Fe on the predicted $[Fe(CN)_6]^{4-}$ spectrum

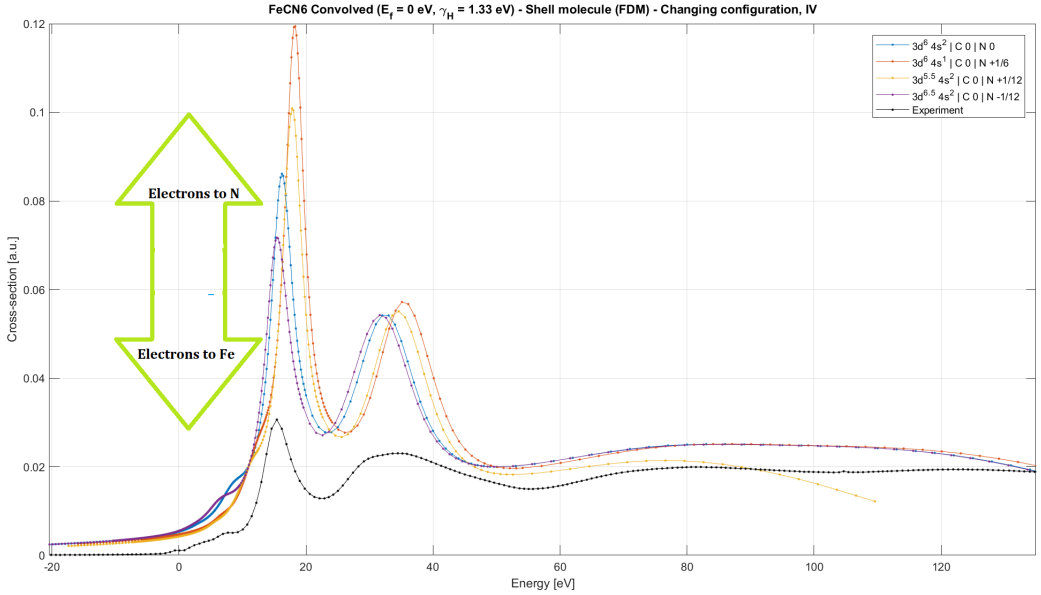

Figure 16: Effects of charge transfer between N and Fe on the predicted $[Fe(CN)_6]^{4-}$ spectrum

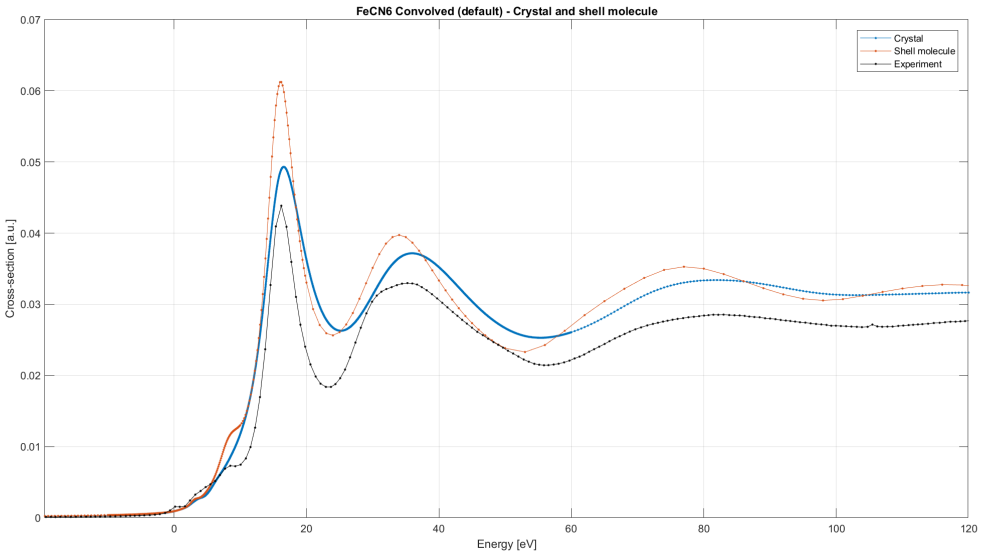

Figure 17: Predicted and experimental spectra for $[Fe(CN)_6]^{4-}$ with the default convolution

5.2 $[Fe(Terpy)(CAB)]^{2+}$

This compound, which I shall call $[Fe(Terpy)(CAB)]^{2+}$, could be better described as iron para-pyridil-terpyridine carbene (see figure 26). It is an intermediate compound in the syntesis of $[Fe(CAB)_2]2+$ from iron terpyridine.
I have run calculations with the crystallographic structure, and with two structures calculated using the PBE density functional: $[Fe(Terpy)(CAB)]^{2+}$ in gas phase, and $[Fe(Terpy)(CAB)]^{2+}$ in an acetonytrile (ACN) solution.
The results are shown in figure 27. The spectra predicted using the DFT structures are very close, while the crystallographic one is slightly lower than the other two. All the spectra have a declining shoulder, where in the experiment there is a second peak. Experience with cyanides suggests that the height in this point can not be varied changing the configuration of the molecule. Neither can we modify the convolution, at least if we want $\Gamma(E)$ to be monotonically increasing in this region, because we would obtain an unrealistic bunch a bit after the main edge.
What we can do is to lower the first peak: in this way we would have the right aspect for the XANES spectrum, at the price of an overall lower amplitude with respect to the background. The electrons that the Fe atom has to receive can come from the four near N atoms, from the two C atoms, or from both. As seen in Figure 28, I obtained the closes match with the transfer of 2 electrons from the C ligands.

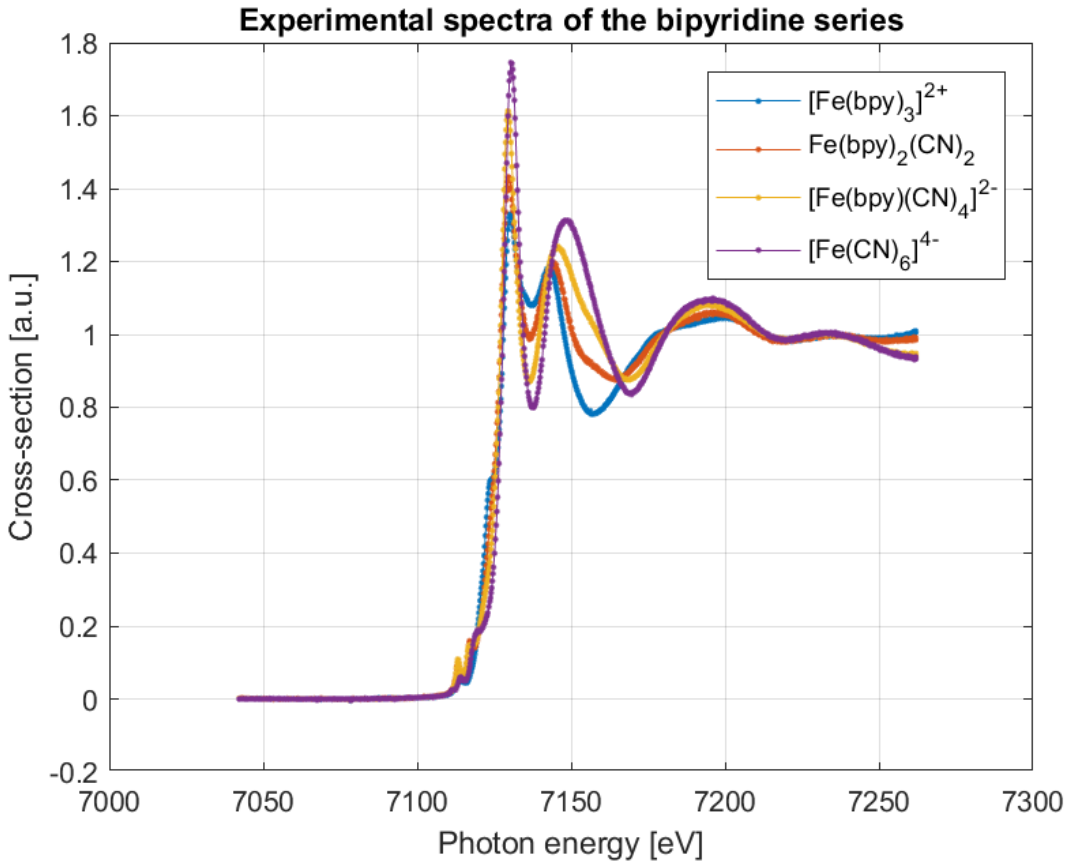

Figure 18: Experimental spectra of the bipyridine-cyanide family

5.3 $[Fe(CAB)_2]^{2+}$

I tested the structure in a crystallographic file, and some structures calculated with the PBE functional for different crystal symmetries. The experimental spectrum of $[Fe(CAB)_2]^{2+}$ features a roughly flat plateau, until 30 eV after the edge. In contrast, in anyone of the predicted spectra the amplitude right after the edge is not equal to the amplitude at the end of the XANES region. I suspect some mislabeling of the DFT structures; anyway, two of the DFT structures lead to a good prediction, and other two not. The calculation based on the crystallographic structure fails miserably. The charge transfer between iron and ligands can vary the first peak, but a middle transition would be required to make the spectrum flat. In figure 30 I tried some displacements of electron between the four C ligands, and the outer N atoms with which they are bounded. Apparently this operation can make the spectrum flat (sometimes with a reasonably sized pre-edge, and sometimes not).

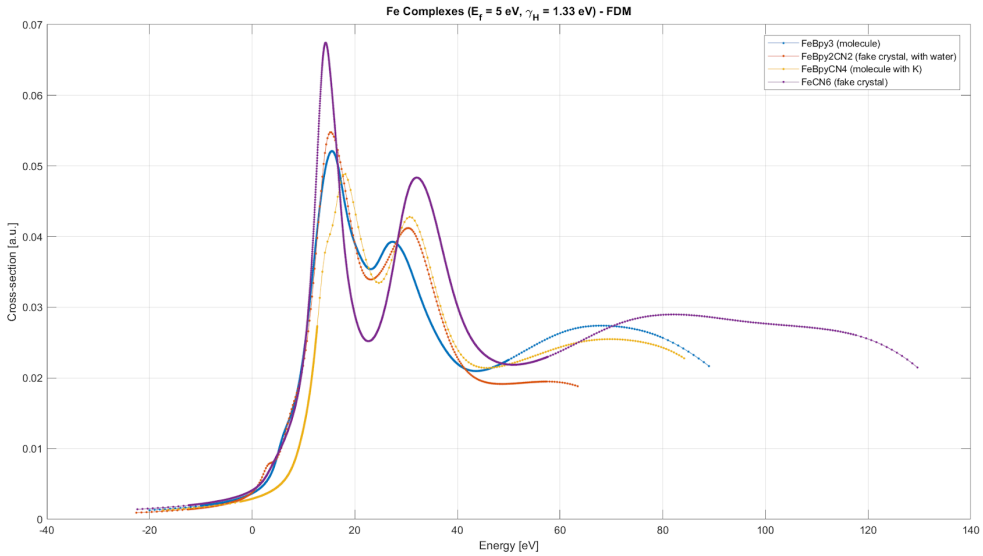

Figure 19: Computed spectra of the bipyridine family, with single-molecule inputs and core-hole convolution. The spectra are shifted as to cross at $\mu = 0.01$ a.u.

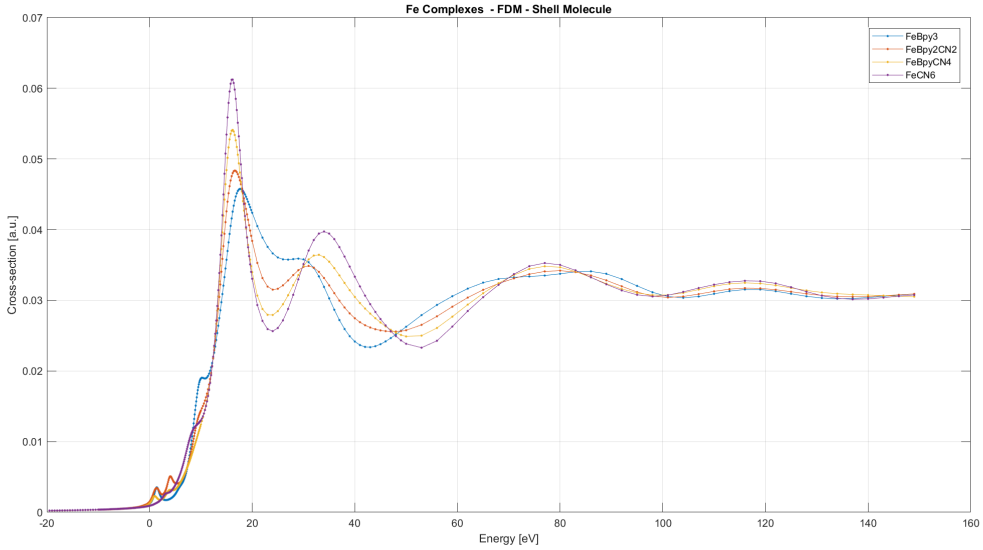

Figure 20: Computed spectra of the bipyridine family, with the default convolution

5.4 Whole series

Figure 31 shows the experimental spectra of this family. While the spectra of the iron cyanide-bipyridine family feature a minimum in the intermediate part of the XANES region, the three compounds in this family mantain an almost constant cross-section. The spectrum of $[Fe(terpy)(CAB)]^{2+}$ is somewhat intermediate between the spectra

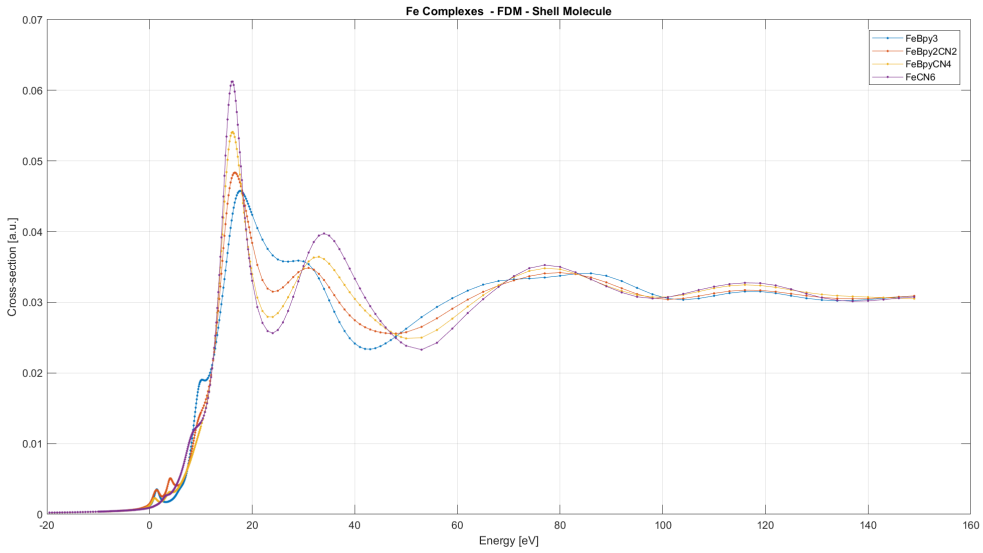

Figure 21: Computed spectra of the bipyridine family, with the core-hole convolution

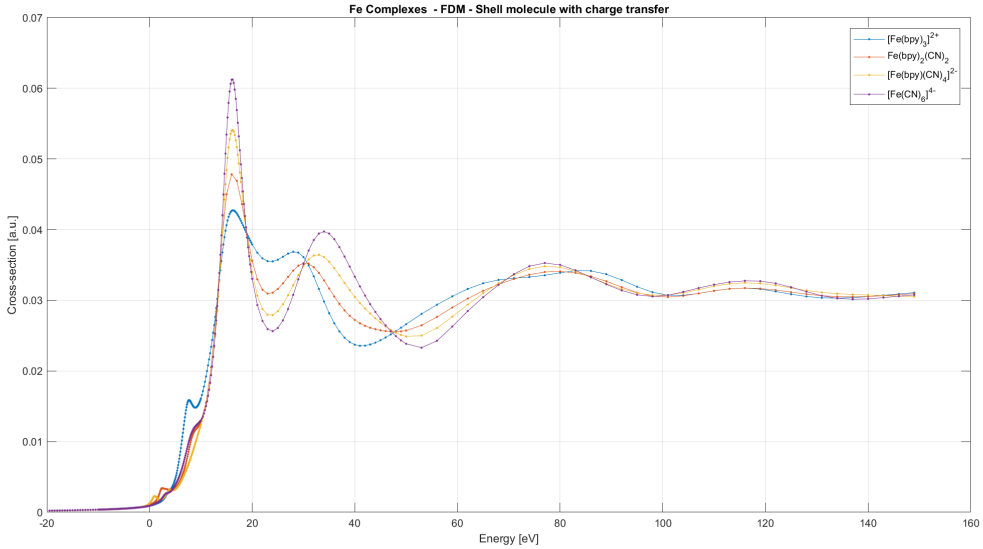

Figure 22: Same option as figure 20, but the iron atom has configuration $3d^8\,4s^0$ in $[Fe(Bpy)_3]^{2+}$, and $3d^{6.7}\,4s^{1.3}$ in $Fe(bpy)_2(CN)_2$

of $[Fe(terpy)_2]^{2+}$ and $[Fe(CAB)_2]^{2+}$. Unlike in the bipyridine family, there seems to be some nodal points in the EXAFS region, but not in the XANES region. The three computed spectra cross are close to each other, like the experimental ones, but the shape of the XANES region is not correct. Moreover, they have a shoulder at ~ 40 eV whereas the real spectra are flat.

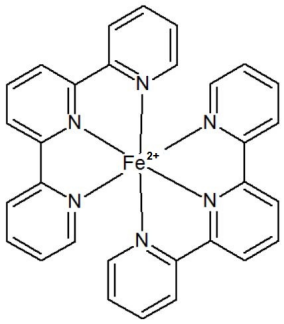

Figure 23: Structural formula of iron(II) bi-(2,2,2)terpyridine

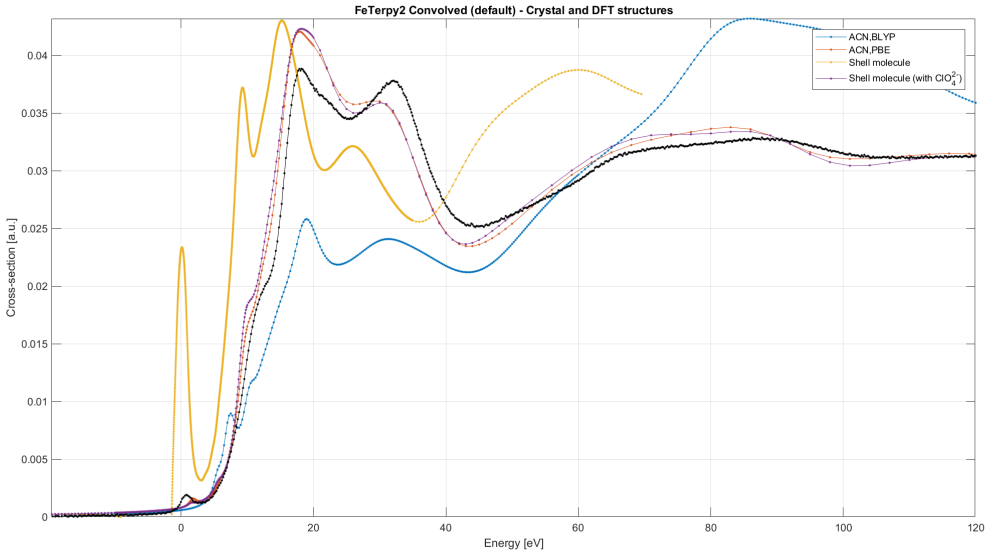

Figure 24: Predicted and experimental spectra for $[Fe(Terpy)_2]^{2+}$

6 Conclusions

The software *FDMNES* can successfully predict the qualitative features of the X-ray absorption near edge structure spectra of the iron(II) complexes in the bipyridine and carbene families The Muffin Tin method always returned less accurate results, but thanks to its rapidity it could be used for exploration purposes. The best way to construct the input structure is to include all the atom inside the volume that the program uses for the calculation.
The region of the spectrum within the first ∼10 eV after the K edge depends critically on the distribution of electrons in the molecule: generally, moving electrons toward the center lowers the absorption cross-section in that region, and vice versa. The changes in the internal configuration of external atoms do not affect the spectra in an appre-

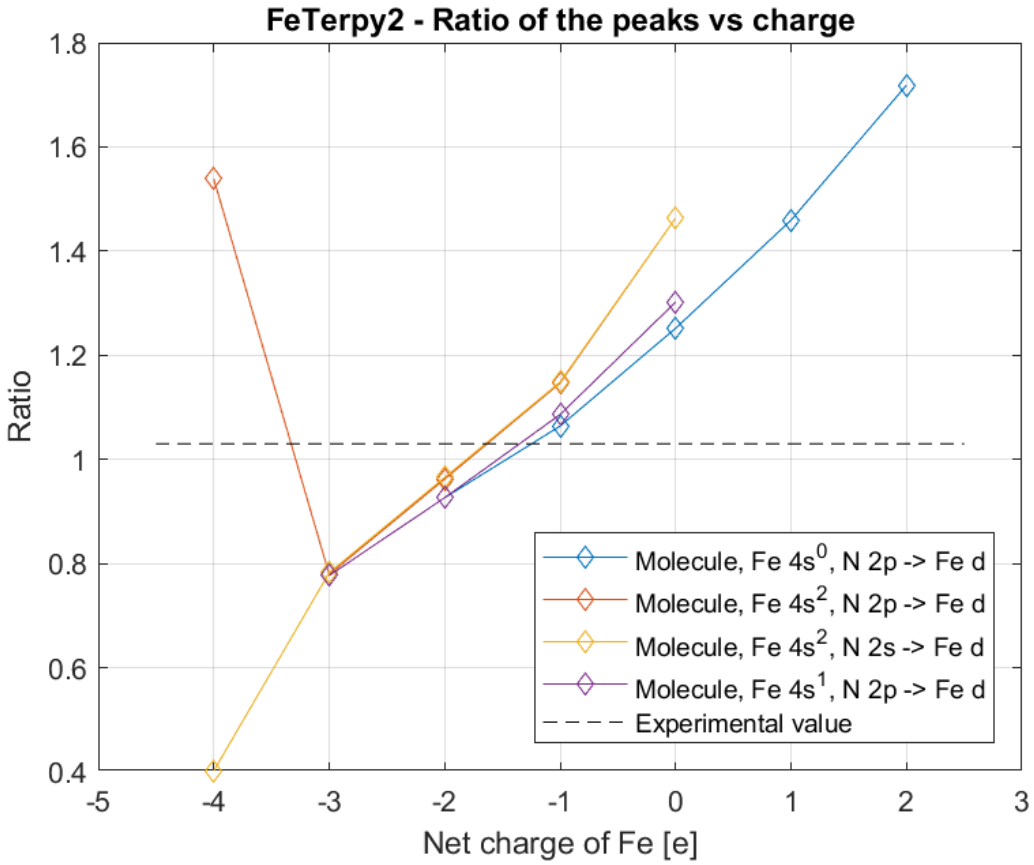

Figure 25: Ratio between the first and the second peak of the $[Fe(Bpy)_3]^{2+}$, for various electronic configurations

ciable manner. The intermediate region, between ∼10 eV and ∼25 eV, seems to be less sensitive to configuration changes, but at least in one case it is affected by charge transfer between the external atoms. Finally, the region between ∼25 eV and ∼40 eV after the edge, before the signal fades into EXAFS, is untouched by all charge transfer I have tried. The cross-section in this region seems to decrease only if we increase the length of the bonds between iron and the ligands. Thanks to its insensitiveness to the electronic configuration, the height of this region can perhaps be used to decide the convolution function, i.e., to assess the contribution to the broadening of inelastic scattering processes.

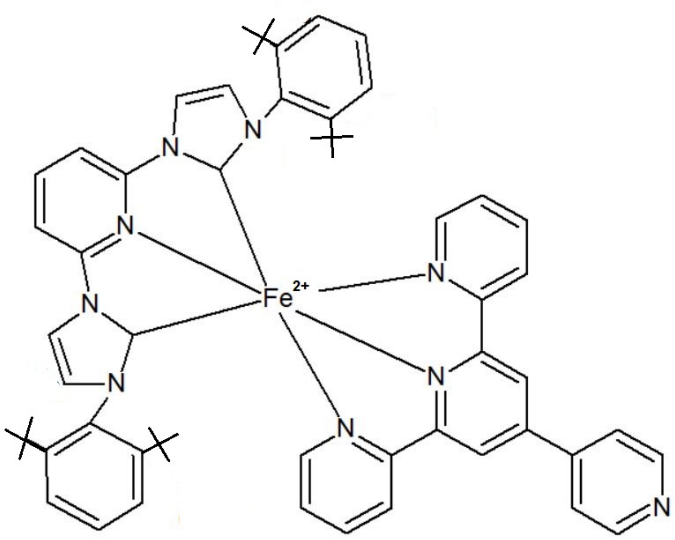

Figure 26: Structural formula of $[Fe(Terpy)(CAB)]^{2+}$

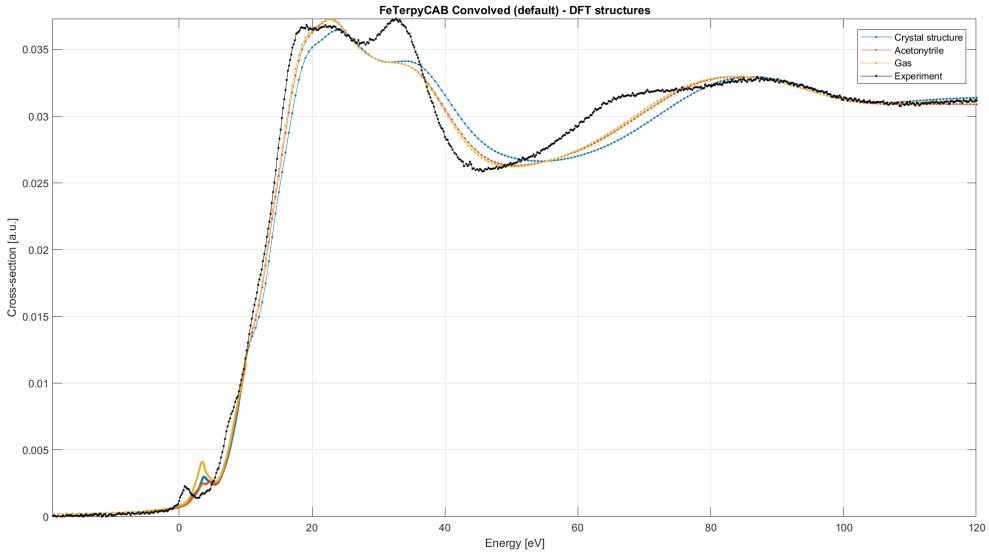

Figure 27: Predicted and experimental spectra for $[Fe(Terpy)(CAB)]^{2+}$

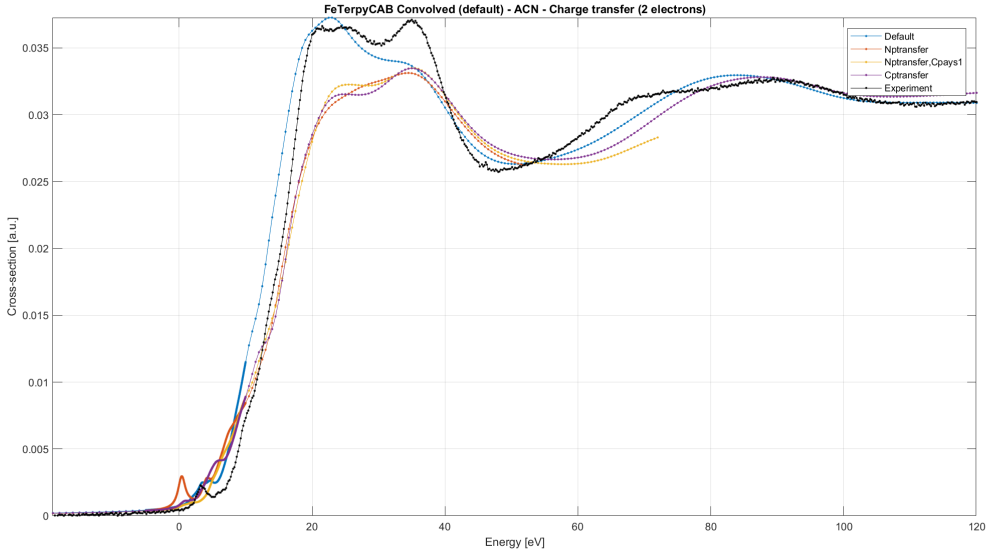

Figure 28: Effect of the donation of two electrons from ligands on the spectrum of $Fe(Terpy)(CAB)$

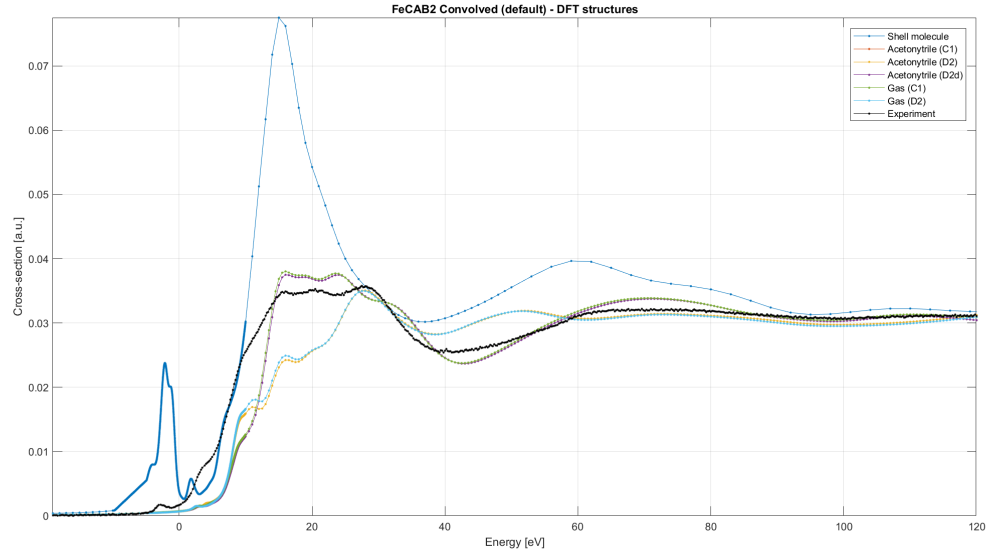

Figure 29: Predicted and experimental spectra for $[Fe(CAB)_2]^{2+}$

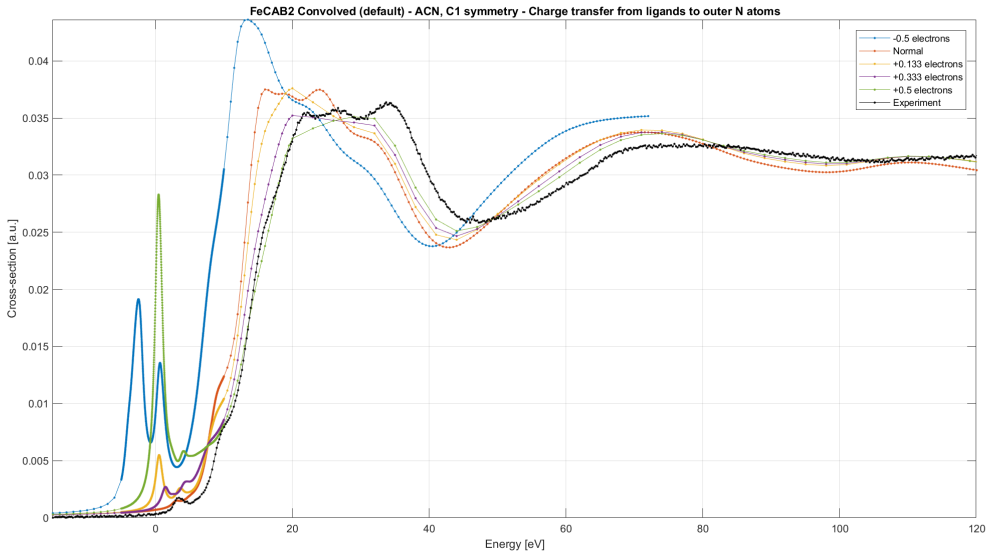

Figure 30: Effect of the transfer of electrons between C ligands and outer N atoms on the spectrum of $Fe(CAB)_2$

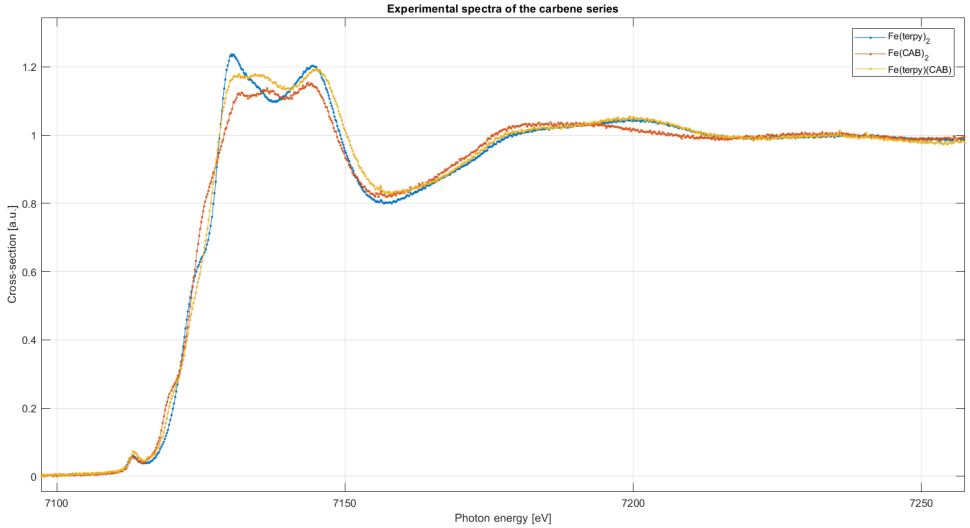

Figure 31: Experimental spectra of the terpyridine-carbene family

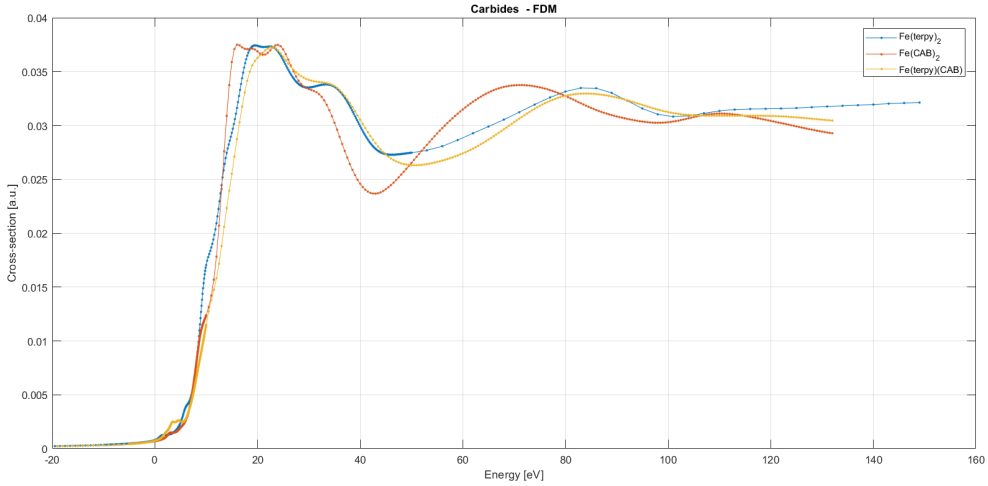

Figure 32: Computed spectra of the terpyridine-carbene family, with the default convolution

References

[1] M.Abrahmson, *Solar energy conversion using iron polypiridil type fotosentitizers - a viable ruote for the future?*, Photochemistry (2017) **44**: 285-295

[2] E. Galoppini, *Strike while the iron is cold*, Nature Chemistry (2015) **7**: 861-862

[3] M.Neville, *Fundamentals of XAFS*, Reviews in Mineralogy and geochemistry (2004) **78**(1)

[4] Y. Joly (2008), *FDMNES User's Guide*: https://www.uow.edu.au/~/greg/html/Manuel_Eng.pdf

[5] Y. Joly, S. Grenier (2015), *Theory of X-Ray Absorption Near Edge Structure*, in *X-Ray Absorption and X-Ray Emission Spectroscopy: Theory and Applications*, John Wiley & Sons, ISBN 9781118844281